Influence of the Ambient Pressure on the Weld Quality for Magnetic Pulse Welded Sheet Joints

S. Kümper[1*], E. Schumacher[1], S. Böhm[1]

[1] Department for Cutting and Joining Manufacturing Processes, Institute for Production Technologies and Logistics, University of Kassel, Germany
*Corresponding author. Email: s.kuemper@uni-kassel.de

Abstract

This paper examines the effect of reduced ambient pressure during the welding process on the quality of magnetic pulse weld seams. For this purpose, a specifically developed vacuum chamber was applied, which enables a reproducible implementation. This, in turn, prepared the ground for a systematic examination of this promising process parameter. The tests focused on comparison of the weld seams realized with different currents and acceleration distances under atmospheric pressure and in the vacuum chamber. Here, both similar (EN AW-1050-H14) and dissimilar material combinations were considered (EN AW-1050A-H14 + S235JR; EN-AW 6016-T6 + DC04). The evaluation criteria for the quality of the welds were the tensile strength of the joint and the size of the weld seam.

Keywords

Magnetic Pulse Welding, Aluminium, Steel

1 Introduction

In many industrial sectors, hybrid joining of different materials are in great demand for combining the advantages of each material. In this case new, resource-conserving and sustainable manufacturing processes come to the fore (Garg et al. 2016). For the combination of high strength with low specific weight, especially aluminum-steel-connections are interesting, but conventional fusion welding processes are limited for joining these material combinations. Alternative joining processes like screw technology, riveting or bonding are often not suitable because of their negative influence on the total

weight (screwing / riveting) or their usually long process times (bonding) (Hahn et al. 2016).

The process of magnetic pulse welding (MPW) enables the joining of different materials with high strength of the welded joint. With this process, the joining of aluminum with steel, copper, titanium, magnesium and polyurethane as well as the joining of copper with brass or amorphous glass was possible (Patra et al. 2017, Raoelison et al. 2012). Although the intensely research in the field of MPW started at the End of the 20th century and though even today not all appearing mechanism can be explained adequate, the process of MPW is used in a multiplicity of sectors of industry: automotive industry (e.g. lightweight construction, exhaust system, fuel filter), aerospace engineering (e.g. mechanical aircraft steering, shafts) or electrical engineering (e.g. bonds, board coatings, wire connection) (Kapil and Sharma 2015, Groche et al. 2017). A process parameter, which is nowadays in the focus of research, is the ambient pressure of the mating parts during the joining process. Referring to Pabst and Groche (2016 and 2018), the ambient pressure and the surrounding gas during the process can be used to improve the weld quality: by reducing the ambient pressure or changing the surrounding gas, an effect on the weld seam quality and influence on the joining mechanism are observable. The aspect of ambient pressure should be considered in detail in the following article.

2 Experimental Setup

2.1 Magnetic pulse welding

A MPW-system “PSTproducts BlueWave 48-16” was used for this study, which generally consists of two components: a capacitor bank and a tool coil. The present system allows a maximum discharging energy of E = 48 kJ and a maximum discharging voltage of U = 16 kV. For the joining process, the one-turn flat coil B80/10 was used, which offers a usable coil length of 80mm and a coil width of 10 mm. During the joining process, a high current pulse (f ≈ 18 to 19 kHz) is conducted through the coil, which is forming a magnetic field, inducting a current flow to the loose flyer sheet. By this current flow, a second magnetic field is formed around the flyer sheet, accelerating this loose sheet in the direction of the fixed target sheet. The flyer gets accelerated across an adjusted distance (gap) and hits the target with high velocity and high pressure, which results in a welded joint between these two parts. For inducting the current flow to the loose flyer sheet, it has to be a good electrical conductor. A schematic representation of the process is shown in **Figure 1**.

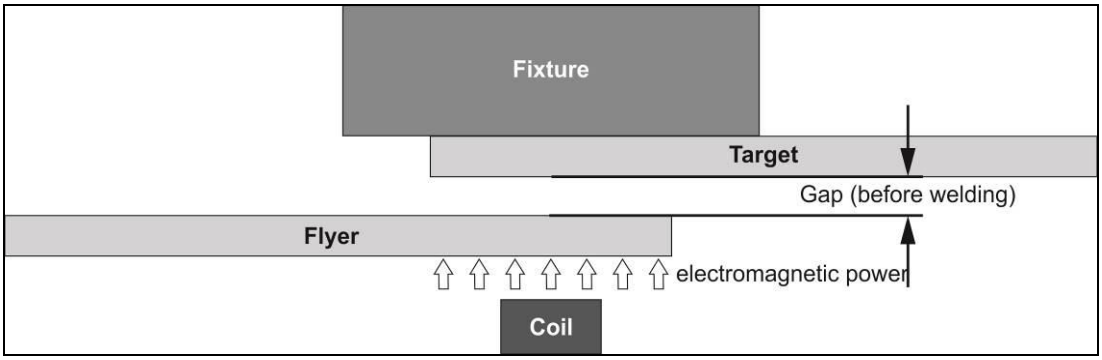

Figure 1: *Schematic representation of the MPW-process*

2.2 Vacuum Chamber

The grounded vacuum chamber (see

Figure *2*, left) was developed at the Department for Cutting and Joining Manufacturing Processes and is built of stainless steel (1.4301). The chambers cover consists of aluminum EN AW-5083 with an ISO-K-clamping flange connection according to DIN 28404. Below the chamber, the MPW-coil is integrated into a base plate, composed of constructions plastics (POM C). The target is clamped by two toggle levers, which are connected to the base plate by glass fiber reinforced plastics (see

Figure *2*, right).

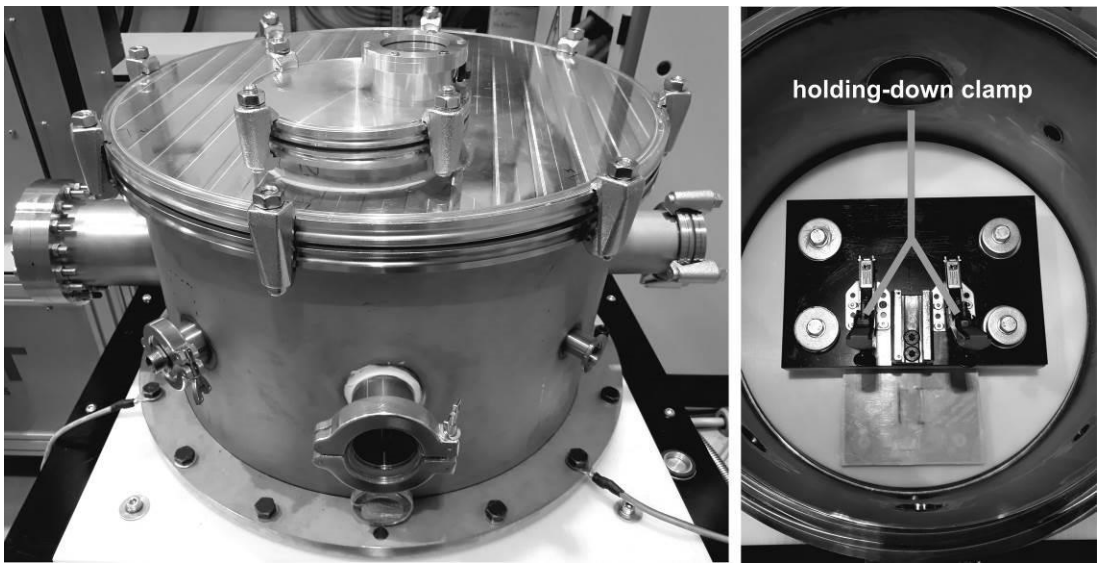

Figure 2: *vacuum chamber designed for MPW (left: vacuum chamber with cover, right: coil and holding-down clamp)*

The evacuation of the chamber is realized by a rotary vane pump Leybold TRIVAK D4B. The vacuum is measured by a Leybold IONIVAC-transmitter ITR 90, covering a measurement range of $p = 5x10^{-5}$ to $1x10^{3}$ mbar. The reproducible and with the present experimental setup achievable vacuum is located in the range of p = 30 to 100 mbar (low vacuum). During the welding process, the pressure inside the vacuum chamber has been kept constant. By the use of the vacuum chamber, the discharge frequency is reduced from f ≈ 19,6kHz (without vacuum chamber) to f ≈ 18,4kHz (with vacuum chamber).

2.3 Experimental Materials

For this research, similar and dissimilar material combinations were chosen. As a similar combination the aluminum EN AW-1050-H14 was used. For the examination of the influence on dissimilar combinations, two different aluminum-steel-combinations were tested. As first combination, aluminum EN AW-1050-H14 was welded with a mild steel S235JR. The second combination was the automotive alloy EN AW-6016-T6 joined with a deep drawing steel DC04. Important material properties, which were determined before the study, are presented in
Table *1*. All sheets have the dimensions of 40 mm x 100 mm and were welded with an overlap of 30 mm.

Material	Thickness [mm]	Tensile strength [MPa]
EN AW-1050-H14	1,5	110
EN AW-6016-T6	1,25	271
S235JR (1.0038)	1,5	344
DC04 (1.0338)	1,5	317

Table 1: *selected material properties*

3 Experimental Setup

3.1 Experimental Parameters

At first, experimental series at atmospheric pressure (p ≈ 1000 mbar) were carried out (below: non-vacuum-welded specimen). Therefor the discharging energy (i.e. discharging current) was successive increased with different accelerating distances (e.g. d = 1 mm / d = 1,5 mm / d = 2 mm). The discharging energies were selected according to the welded materials: the similar material combination EN AW-1050-H14 was welded with discharging energies of E = 8 to 16 kJ (i.e. I = 230 to 340 kA), the dissimilar material combinations were welded with E = 9 to 15 kJ (i.e. I = 250 to 330 kA) for the combination of EN AW-1050-H14 with S235JR and E = 13 to 21 kJ (i.e. I = 305 to 395 kA) for the combination EN AW-6016-T6 and DC04. Afterwards, experiments with reduced pressure

(p = 30 to 100 mbar) and identical discharging energies and accelerating distances were executed (below: vacuum-welded specimen).

3.2 Weld Seam Analysis

The welded sheets were tested and rated on their maximum tensile strength. Additionally, the local characteristic and size of the weld seam area was evaluated to get information about the beginning of the joining. For this evaluation, the specimen, which failed in the weld seam during tensile strength testing, were light microscopically analyzed and measured. This light microscopic analysis was performed with a Leica Z16APOA microscope and the associated software Leica Application Suite V4.8.

For the measurement of the weld seam size, the welded area on the target sheet was examined in a top view after tensile strength testing. The target sheet was analyzed with the software named before and the weld seam area was generated by building the difference of the area defined by the outer weld seam edge and the area of the inner ellipse, where no weld could be examined.

4 Results

4.1 Tensile strength

Specimen of the similar material combination EN AW-1050-H14, which failed in the base material, were able to sustain F = 5800 N tensile force. The comparison of sustainable tensile forces of vacuum- and non-vacuum-welded specimen shows a positive influence on the strength of the weld by welding under vacuum: For equal discharging energies (i.e. discharging currents) vacuum-welded specimen show a higher strength than non-vacuum-welded specimen. Moreover, the discharging energy, at which the failure takes place in the base material, is lower for vacuum-welded specimen (E ≈ 10 kJ) than for non-vacuum-welded specimen (E ≈ 14 kJ).
Figure 3 shows the results of the tensile strength test.

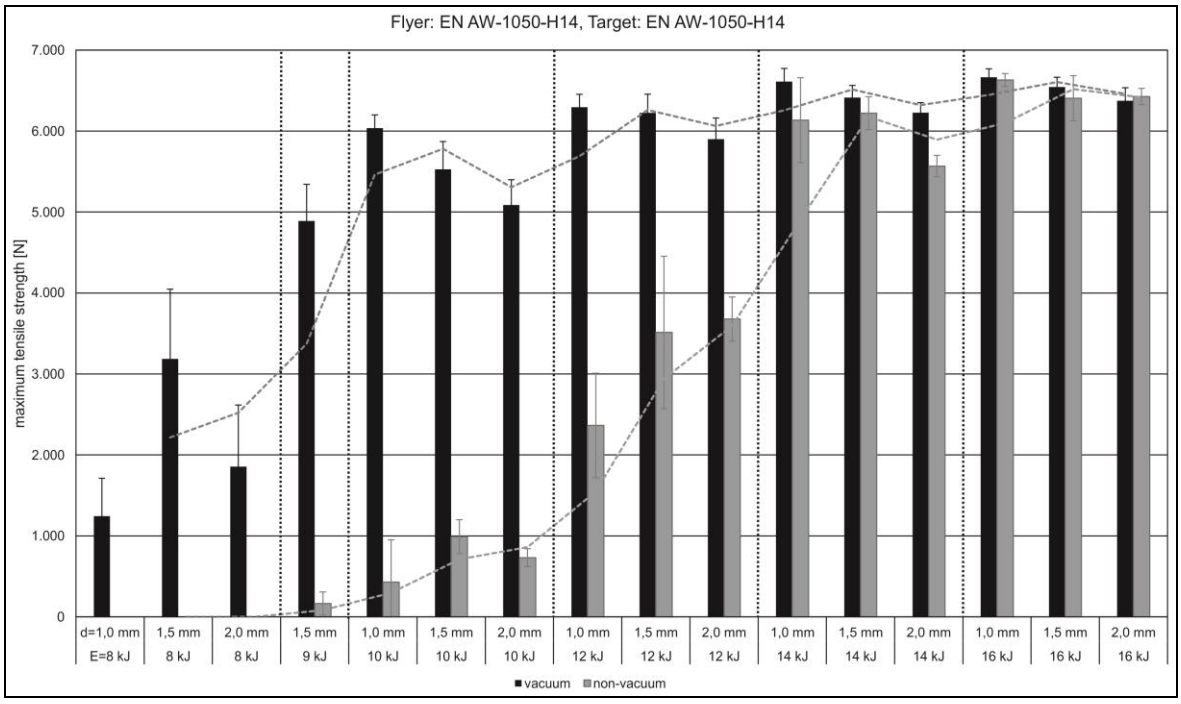

Figure 3: *maximum tensile strength of vacuum- (black) and non-vacuum-welded (grey) specimen (similar material combination EN AW-1050-H14)*

The dissimilar material combination EN AW-6016-T6 and DC04 also shows a movement of the lower process window to lower discharging energies when welding was executed with reduced ambient pressure. This material combination could be welded at discharging energies of E = 13 kJ under vacuum, whereas non-vacuum specimen could only be welded with discharging energies higher than E = 16 kJ. Usually vacuum welded specimen show higher tensile strengths and lower variations in their tensile strength at comparable discharging energies and accelerating distances. At discharging energies of E = 21 kJ, vacuum-welded and non-vacuum-welded specimen have a similar tensile strength by comparable variation, as
Figure 4 shows. The second dissimilar material combination (EN AW-1050-H14 and S235JR) also shows a movement of the lower process window of vacuum-welded specimen compared to non-vacuum-welded to lower discharging energies, but not as clearly as it could be observed at the combination EN AW-6016-T6 and DC04. When welded under vacuum, specimen could be joined at discharging energies of E = 9 kJ and accelerating distances of d = 1 mm. Compared to that, non-vacuum-welded specimen could be joined at E = 9 kJ / d = 1,5 mm and E = 10 kJ / d = 1 mm.

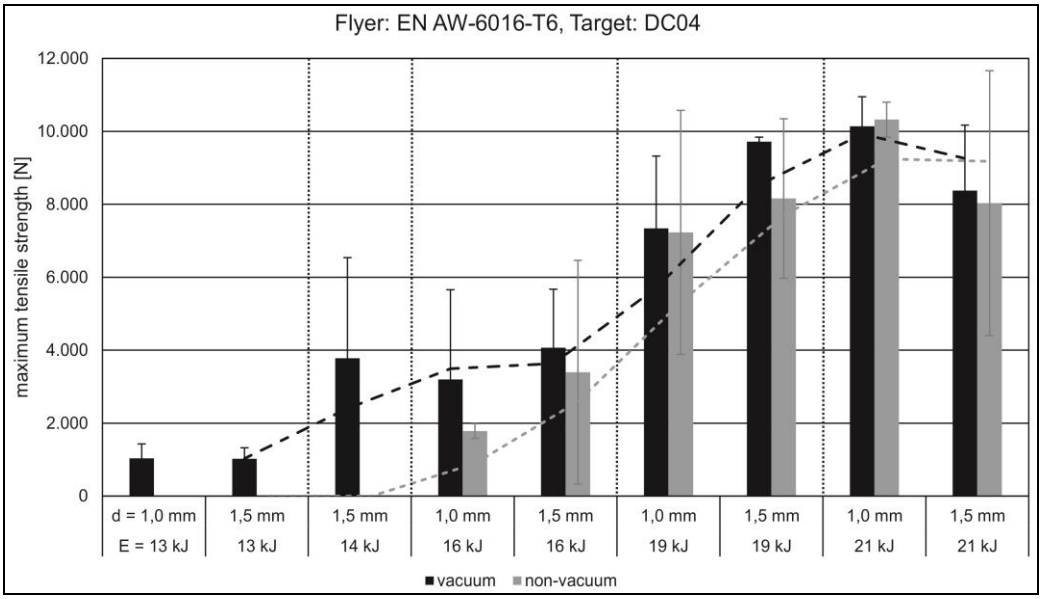

Figure 4: *maximum tensile strength of vacuum- and non-vacuum-welded specimen (EN AW-6016-T6+DC04)*

4.2 Weld seam area

By comparing the weld seam area, it is obvious, that there is a better and bigger weld seam shape when the specimens were welded with reduced ambient pressure.
Figure 5 shows the comparison of the similar material combination EN AW-1050-H14, welded with the same process parameters (E = 8 kJ, I = 233 kA, d = 1,5 mm). It becomes apparent, that the weld seam is better formed at pressures p < 100 mbar (see
Figure 5, bottom). When welded under vacuum, particle of the flyer material (respectively the target material) can be examined on the other joining partner. At atmospheric pressure, only an imprint can be observed.

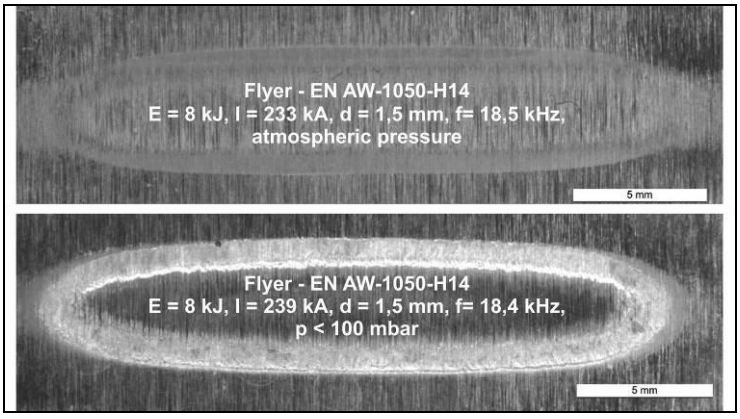

Figure 5: *comparison of vacuum-welded (bottom) and non-vacuum-welded (above) specimen. At atmospheric pressure, no successful weld was possible.*

Figure 6 shows the measured weld seam area of vacuum- and non-vacuum-welded specimen for the dissimilar material combination EN AW-6016-T6 and DC04. The diagram illustrates the larger weld seam areas for vacuum-welding at equal process parameters, compared to welding at ambient pressure. In addition to that, the variation of the weld seam area is smaller when the specimens are welded under vacuum.

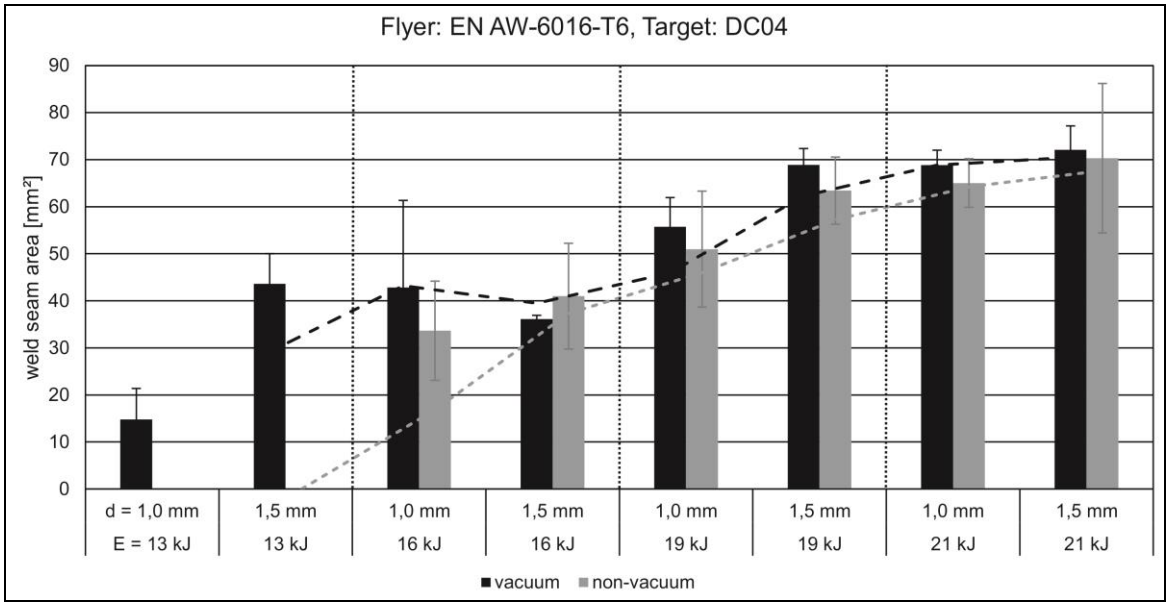

Figure 6: *weld seam area of vacuum- and non-vacuum-welded specimen (EN AW-6016-T6+DC04)*

5 Conclusion

The presented investigation shows the positive influence of a reduced ambient pressure on the tensile strength of magnetic pulse welded joints. This influence could be pointed out by welding the similar material combination EN AW-1050-H14 and the dissimilar material combinations EN AW-1050-H14 + S235JR and EN AW-6016-T6 + DC04 with the process of magnetic pulse welding. Based on the process parameters, a successful welding was possible at lower discharging energies (i.e. discharging currents) when the welding was performed under vacuum. Successful welding processes could be performed at discharging energies of E = 13 kJ under vacuum, whereas discharging energies of E = 16 kJ were needed for welding at ambient pressure (EN AW-6016-T6 + DC04, see **Figure 4** and **Figure 6**). A reduction of the ambient pressure also provides an opportunity to reduce the discharging energy, at which the beginning of the welding process could be observed (i.e. lower process window). This effect could be recognized by welding similar as well as

dissimilar material combinations. Simultaneous the discharging energy, at which the failure of tensile shear testing takes place in the weaker base material, could be decreased by magnetic pulse welding with reduced ambient pressure.

In addition to the increase of tensile strength, an enlargement of the weld seam area at similar process parameters could be observed. This influence can be used to explain the gain of tensile strength by enlarging the area for strain transmission. At this point it could be supposed that the forming of the weld seam begins earlier and stops later when the ambient pressure was reduced. Referring to Bergmann et al. (1966) and Deribas and Zakharenko (1974), a certain relationship between the jet velocity and the collision velocity has to exist to enable the forming of an explosion welded weld seam. Based on this perception, the required relationship could be achieved earlier when the magnetic pulse welding takes place at reduced ambient pressure, where a lower air resistance exists. This aspect of higher velocities, depending on the ambient gas densities, could also be noticed by Pabst and Groche (2018), when magnetic pulse welding was executed with different ambient gases.

Further investigations and detections on the collision conditions have to be performed to deepen this boundary condition of magnetic pulse welding and to explain the influence of the jet on the bonding mechanism. Collision velocities and collision angles have to be defined to characterize the influence of the ambient pressure on the collision conditions and thereby characterizing their influences on the bonding mechanism.

References

Bergmann, O. R., Cowan, G. R., Holtzman, A. H., 1966. *Experimental Evidence of Jet Formation During Explosion Cladding*. Transactions of the Metallurgical Society of Aime, 236, pp. 646-653.

Deribas, A. A., Zakharenko, I. D., 1974. *Surface effects with olique collisions between metallic plates*. Combustion, Explosion and Shock Waves, 10, pp. 358-367.

Garg, A., Panda, B., Shankhwar, K., 2016. *Investigation of the joint length of weldment of environmental-friendly magnetic pulse welding process.* The International Journal of Advanced Manufacturing Technology 87, pp. 2415-2426.

Groche, P., Becker, M., Pabst, C., 2017. *Process window acquisition for impact welding processes*. Materials & Design 118, pp. 286–293.

Hahn, M., Weddeling, Ch., Taber, G., Vivek, A., Daehn, G.S., Tekkaya A.E., 2016. *Vaporizing foil actuator welding as a competing technology to magnetic pulse welding.* Journal of Materials Processing Technology 230, pp. 8-20.

Kapil, A., Sharma, A., 2015. *Magnetic pulse welding: An efficient and environmentally friendly multi-material joining technique.* Journal of Cleaner Production 100, pp. 35–58

Pabst, C., Groche, P., 2016. *The Influence of Thermal and Mechanical Effects on the Bond Formation During Impact Welding.* In: Tekkaya, A.E., Kleiner, M. (Eds.), High Speed Forming 2016, Proceedings of the 7th International Conference, Dortmund, Germany, pp. 77-88.

Pabst, C., Groche, P., 2018. *Identification of Process Parameters in Electromagnetic Pulse Welding and Their Utilisation to Expand the Process Window.* In: International Journal of Materials, Mechanics and Manufacturing, 6 (1), pp. 69-73.

Patra, S., Arora, K.S., Shome, M., Bysakh, S., 2017. *Interface characteristics and performance of magnetic pulse welded copper-steel tubes*. Journal of Materials Processing Technology 245, pp. 278–286.

Raoelison, R. N., Buiron, N., Rachik, M., Haye, D., Franz, G., 2012. *Efficient welding conditions in magnetic pulse welding process.* Journal of Manufacturing Processes 14, pp. 372–377